analytical chemistry

pubs.acs.org/ac Article

# Nanosecond Laser Ablation–Multicollector Inductively Coupled Plasma-Mass Spectrometry for in Situ Fe Isotopic Analysis of Micrometeorites: Application to Micrometer-Sized Glassy Cosmic Spherules

Claudia González de Vega, Marta Costas-Rodríguez, Thibaut Van Acker, Steven Goderis, and Frank Vanhaecke*

Cite This: *Anal. Chem.* 2020, 92, 3572–3580 Read Online

ACCESS | Metrics & More | Article Recommendations | Supporting Information

**ABSTRACT:** This work evaluates the use of nanosecond laser ablation–multicollector inductively coupled plasma-mass spectrometry (ns-LA–MC-ICP-MS) for Fe isotopic analysis of glassy cosmic spherules. Several protocols for data acquisition from the transient signals were compared, with the integration method, i.e., isotope ratios obtained by dividing the corresponding signal intensities integrated over the selected signal segment, providing the best precision. The bias caused by instrumental mass discrimination was corrected for by a combination of internal correction using Ni as an internal standard (coming from a conebulized standard solution) and external correction using a matrix-matched standard. Laser spot size and repetition rate were adapted to match the signal intensities for sample and standard within ±10%. For in situ isotopic analysis, the precision of the $\delta^{56}$Fe values ranged between 0.02 and 0.11‰ (1 SD, based on 4 measurement sessions, each based on ablation along 5 lines for 30 s each) and 0.03–0.17‰ (SD, based on 3 measurement sessions) for glass reference materials and micrometeorites, respectively. Despite this excellent reproducibility, the variation of the isotope ratios along a single ablation line indicated isotopic inhomogeneity exceeding 1‰ in some micrometeorites. Isotopic analysis via pneumatic nebulization MC-ICP-MS, after sample digestion and chromatographic Fe isolation, was performed to validate the results obtained by in situ isotopic analysis, and good agreement was achieved between the $\delta$-values obtained via both approaches and with those reported in literature for MPI-DING and USGS glass reference materials. Also for the glassy cosmic spherules, overall, there was a good match between the ns-LA–MC-ICP-MS and solution MC-ICP-MS results.

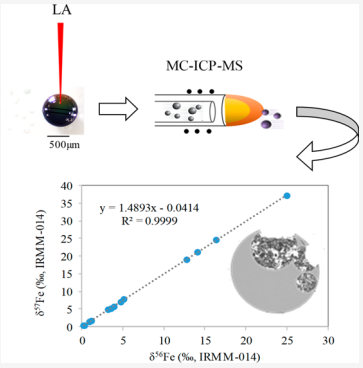


The characterization of extraterrestrial materials, such as meteorites and meteorite phases, e.g., glass, olivine, pyroxene, and Fe–Ni metal, and materials from sample-return missions, is a major driver for the development of novel and powerful analytical methods.[1] Advances in instrumentation, along with the parallel development of proper data acquisition and data-handling strategies, have given rise to a spectacular growth of analytical applications of mass spectrometric techniques in this context. For high-precision isotopic analysis, multicollector inductively coupled plasma-mass spectrometry (MC-ICP-MS) is the technique most commonly used nowadays, as it combines a high ionization efficiency and high sample throughput with sufficient precision to reveal the sometimes very small differences in isotope ratios caused by relevant processes.[2,3] Several works focused on the topic of Fe isotope geo- and cosmochemistry have been carried out using MC-ICP-MS already.[4,5] The isotopic composition of Fe was already determined in a wide range of Fe-bearing materials and matrices, including chondrites[6] and iron meteorites.[7,8] Dauphas et al.[9] obtained accurate Fe isotope ratio results for geological materials with a precision <0.03‰ on the $\delta^{56}$Fe value using (pseudo-high mass resolution) MC-ICP-MS after sample digestion and target element isolation.

The combination of solid sampling via laser ablation (LA) with MC-ICP-MS provides direct isotopic information, while avoiding sample pretreatment and reducing the sample consumption.[10] Previously, femtosecond (fs)-LA–MC-ICP-MS has been successfully applied for that purpose in a variety of mineral matrices,[11,12] e.g., iron metal, sulfides, hematite, siderite, goethite, magnetite, and silicates.[13] Oeser et al.[14] reported in situ Fe isotopic analysis of reference glass materials using fs-LA–MC-ICP-MS, proving that the spatial resolution and precision achievable were suitable to resolve the diffusion-generated Fe–Mg isotopic zoning in magmatic olivines. Also separate mineral phases of such samples can be studied. In this context, the Fe isotopic composition has already been used to

Received: September 3, 2019
Accepted: February 4, 2020
Published: February 4, 2020

Downloaded via UNIV LIBRE DE BRUXELLES on March 10, 2023 at 14:29:32 (UTC).
See https://pubs.acs.org/sharingguidelines for options on how to legitimately share published articles.

ACS Publications © 2020 American Chemical Society



https://dx.doi.org/10.1021/acs.analchem.9b04029
*Anal. Chem.* 2020, 92, 3572–3580

provide insights into geo- and cosmochemical processes, such as fractional crystallization and planetary core formation.[15]

One of the major issues of in situ elemental and isotopic analysis via LA−ICP-MS is securing accuracy. The occurrence of elemental fractionation during aerosol formation, aerosol transport, and ICP-related processes, e.g., atomization and ionization, needs to be adequately addressed. In addition to elemental fractionation, isotope fractionation processes also occur,[16,17] such that for reliable isotopic analysis, proper correction for this phenomenon is required. Additionally, extracting reliable isotope ratio data from short transient signals can be challenging. Some authors have reported that the isotope ratio drift encountered in the case of short transient signals can be corrected for by taking into account the differences in response times between Faraday cups or between a Faraday cup and an ion counter[18] or by correcting the values for the slow response of the Faraday preamplifier.[19] Therefore, strategies to correct for instrumental mass discrimination in LA−MC-ICP-MS and the effects of relevant interferences need to be evaluated.[20] Although nanosecond-based LA systems are more susceptible to matrix effects and isotope fractionation than femtosecond-lasers,[21] improvements in the instrumentation and correction strategies developed in recent years were able to mitigate these effects and to generate accurate and sufficiently precise isotope ratio results in some contexts.[20,22] Moreover, nanosecond-based LA systems are easier to operate and are more affordable, as a result of which they are considerably more widespread.

In this work, the capabilities of ns-LA−MC-ICP-MS for Fe isotopic analysis of glassy cosmic spherules (micrometeorites with a diameter of 400−800 μm) are demonstrated. The authors propose a new approach for in situ Fe isotopic analysis of glass materials via ns-LA−MC-ICP-MS that was validated via analysis of appropriate reference materials (MPI-DING and USGS glasses). The Fe isotopic composition in geological reference materials and in glassy cosmic spherules was also determined by pneumatic nebulization (PN)−MC-ICP-MS after sample digestion and chromatographic Fe isolation to evaluate the precision and accuracy of the method developed. The instrument settings and data acquisition parameters were optimized in order to adequately handle the transient signals generated by ns-LA, while a combination of internal correction based on the introduction of a conebulized Ni solution into the ICP and external correction using a matrix-matched standard was used to address instrumental mass discrimination.

## ■ EXPERIMENTAL SECTION

**Reagents, Reference Materials, and Samples.** Only high-purity reagents and acids were used throughout the experiments. Trace metal grade nitric acid (67−69%, PrimarPlus, Fisher Chemicals, U.K.) and hydrochloric acid (37%, PrimarPlus, Fisher Chemicals) were additionally purified by sub-boiling distillation in a Savillex DST-4000 acid purification system (Savillex Corporation, MN, USA). Ultrapure 9.8 M hydrogen peroxide acquired from Sigma-Aldrich (Belgium) and Trace metal grade hydrofluoric acid (47−51%) from Seastar Chemicals Inc. (Canada) were used as such for sample preparation. Ultrapure water (resistivity ≥18.2 MΩ cm) was obtained from a Milli-Q Element water purification system (Millipore, France). AG MP-1 strong anion exchange resin (100−200 mesh) purchased from Bio-Rad Laboratories (Belgium) was used for the chromatographic isolation of Fe from the sample digests prior to the PN−MC-ICP-MS measurements.

Geological reference materials (GRMs), including the Max Planck Institut (MPI-DING, Germany) reference glasses KL2-G, ML3B-G, GOR128-G, GOR132-G, ATHO-G, StHs6/80-G, and T1-G, and the United States Geological Survey (USGS, VA, USA) basaltic reference glasses BCR-2G and BHVO-2G, were analyzed to validate the method. These glasses vary from felsic (e.g., 3.27 wt % FeO* and 0.103 wt % MgO for ATHO-G) to mafic compositions (e.g., 9.81 wt % FeO* and 26 wt % MgO for GOR128-G).[23] Thirteen glassy cosmic spherules were obtained from Mount Widerøfjellet in the Sør Rondane Mountains (SRM) of Dronning Maud Land, East Antarctica, and have been previously characterized for their major element concentrations through electron microprobe analysis (EMPA) and for their minor and trace element concentrations via LA−ICP-MS.[24]

In situ Fe isotopic analysis via ns-LA−MC-ICP-MS was performed on these GRMs and glassy cosmic spherules, and Fe isotopic analysis by PN−MC-ICP-MS (after sample digestion and chromatographic Fe isolation) was used for method validation. The isotopic reference material IRMM-014 (Institute for Reference Materials and Measurements, Belgium) was used as an external standard for the isotope ratio measurements by PN−MC-ICP-MS, while for in situ determinations of the Fe isotope ratios using ns-LA−MC-ICP-MS, the USGS reference material BCR-2G was used for this purpose. Ni standard solution, obtained via dilution of a single-element standard stock solution of Ni (1000 mg $L^{-1}$, Inorganic Ventures, The Netherlands), was used for correction for instrumental mass discrimination via internal standardization (for both LA or PN as means of sample introduction), while quality assurance/quality control (QA/QC) samples for evaluation of the Fe isotope ratio measurements by PN−MC-ICP-MS were prepared from a commercially available stock solution of Fe (1000 mg $L^{-1}$, Inorganic Ventures).

**Sample Preparation.** GRMs and glassy cosmic spherules were embedded in epoxy mounts and polished to achieve a flat and smooth surface suitable for LA−MC-ICP-MS analysis. For PN−MC-ICP-MS, glass fragments of about 3−10 mg and cosmic spherules (50−500 μg, i.e., what was left over after LA−MC-ICP-MS analysis) were weighed and taken into solution. Digestion of the samples was performed using a two-step microwave-assisted acid digestion protocol in an MLS-1200 MEGA microwave digestion system (Milestone, Italy). Each step consisted of 30 min of heating in a Teflon vessel at the maximum power of 650 W. First, a mixture (2:1) of $HNO_3$ + HF was used. After evaporation to incipient dryness (at 90 °C), the digestion was continued using a second step with 6 mL of aqua regia (3:1, HCl:$HNO_3$). After cooling down, the vessels were opened, and the solutions were evaporated to incipient dryness at 90 °C again. Finally, the residues were redissolved in 2 mL of 6 M HCl + 0.098 mM $H_2O_2$ for subsequent chromatographic isolation of Fe. The chromatographic separation was performed in 1 mL pipet tips filled with 0.5 mL of AG MP-1 resin, as described elsewhere.[25] A piece of cotton was placed as bed support and another one as stopper. The resin was precleaned with 0.5 mL of 7 M $HNO_3$, 0.5 mL of Milli-Q water, 2 mL of 0.7 M $HNO_3$, and 2 mL of Milli-Q water and conditioned with 4 mL of 6 M HCl + 0.098 mM $H_2O_2$. After sample loading, the matrix was eluted from the column in two steps, first with 2 mL of 9 M HCl and second, with 5 mL of 6 M HCl + 0.098 mM $H_2O_2$. The Fe fraction was


https://dx.doi.org/10.1021/acs.analchem.9b04029
Anal. Chem. 2020, 92, 3572−3580

**Table 1. Instrument Settings for the LA System and MC-ICP-MS Instrument**

| Analyte G2 193 nm ArF* Excimer-Based ns-LA System | | | | | | | | |
|---|---|---|---|---|---|---|---|---|
| pulse width (ns) | | | | | | <5 | | |
| energy density (J $cm^{-2}$) | | | | | | 1.74 | | |
| spot size diameter ($\mu$m) | | | | | | 10−30 | | |
| repetition rate (Hz) | | | | | | 20−45 | | |
| helium carrier gas flow rate (L $min^{-1}$) | | | | | | 0.36 | | |
| dosage (no. shots) | | | | | | 20 | | |
| Neptune MC-ICP-MS Unit | | | | | | | | |
| detector type | faraday cups with $10^{11}$ Ω amplifiers | | | | | | | |
| cool gas flow rate (Ar, L $min^{-1}$) | 15 | | | | | | | |
| auxiliary gas flow rate (Ar, L $min^{-1}$) | 0.7−0.8 | | | | | | | |
| sample gas flow rate (Ar, L $min^{-1}$) | 0.9−1.05 | | | | | | | |
| RF power (W) | 1200 | | | | | | | |
| integration time (s) | 1.049 s (ns-LA); 4.194 s (PN) | | | | | | | |
| interface | jet-type sampling and X-type skimmer cones | | | | | | | |
| ns-LA−MC-ICP-MS Cup Configuration | | | | | | | | |
| L4 | L3 | L2 | L1 | center | H1 | H2 | H3 | H4 |
| $^{53}$Cr | – | $^{54}$Fe + $^{54}$Cr | – | $^{56}$Fe | $^{57}$Fe | $^{58}$Ni + $^{58}$Fe | – | $^{60}$Ni |
| PN−MC-ICP-MS Cup Configuration | | | | | | | | |
| L4 | L3 | L2 | L1 | center | H1 | H2 | H3 | H4 |
| $^{54}$Fe | – | $^{56}$Fe | $^{57}$Fe | $^{58}$Ni + $^{58}$Fe | $^{60}$Ni | – | $^{62}$Ni | – |

then eluted with 6 mL of 1 M HCl and collected in a 15 mL Teflon Savillex beaker. The purified Fe fraction was evaporated to dryness at 90 °C to remove residual chlorides and redissolved in concentrated $HNO_3$. This procedure was repeated twice. The final residue was redissolved in 0.5 mL of 0.42 M $HNO_3$. A procedural blank, treated in the same way as the samples, was included in each batch of samples. All sample manipulations were carried out in a class-10 clean lab (PicoTrace, Germany).

**Instrumentation and Measurements.** An Analyte G2 193 nm ArF*excimer-based ns-LA system (Teledyne Photon Machines Inc., MT, USA), equipped with a prototype low-dispersion ablation cell[26] based on the concept reported on by Van Malderen et al.,[27] coupled to a Thermo Scientific (Germany) Neptune MC-ICP-MS instrument was used throughout this work. A He carrier gas flow rate of 0.36 L $min^{-1}$ was selected to efficiently transport the LA-generated aerosol via polyether ether ketone tubing (PEEK, 1 mm ID and 1.5 m length) to a glass T-piece (5 mm ID), where it was mixed with a PN-generated aerosol containing the internal standard Ni. An airtight fitting was used to connect the LA aerosol transport tubing to the orthogonally oriented inlet of the T-piece. The outlet of the spray chamber was connected to the second inlet of the T-piece, and its outlet was directly connected to the injector inlet of the ICP torch (see Supporting Information Figure S1). The instrument settings and data acquisition parameters were optimized in order to adequately handle the transient signals obtained when using ns-LA (compiled in Table 1).

The MC-ICP-MS instrument was equipped with a high-transmission Jet interface consisting of an X-type Ni skimmer and a Jet-type Ni sampler. Isotope ratio measurements were performed at (pseudo) medium mass resolution ($M/\Delta M \sim 6000$) on the interference-free plateau of the peak in static collection mode, thus avoiding spectral interference from the molecular species present in the plasma (mainly $^{40}Ar^{14}N^+$, $^{40}Ar^{16}O^+$, $^{40}Ar^{16}O^1H^+$, $^{40}Ar^{18}O^+$). The use of wet plasma conditions achieved by mixing the LA-generated and the PN-generated aerosols improved the signal stability, as potential variations caused by differences in plasma loading were mitigated. A Ni standard solution (500 $\mu$g $L^{-1}$ in 3% $HNO_3$) was introduced for internal correction for the instrumental mass discrimination affecting the Fe isotope ratio measurement results. The Faraday cups were positioned for simultaneous detection of the $^{53}$Cr, $^{54}$Cr + $^{54}$Fe, $^{56}$Fe, $^{57}$Fe, $^{58}$Fe + $^{58}$Ni, and $^{60}$Ni ion signals[14] (Table 1). The signal intensity at a mass-to-charge ratio of 54 ($^{54}$Fe + $^{54}$Cr) was corrected for the isobaric interference of $^{54}$Cr using the $^{53}Cr^+$ ion signal intensity and the known natural abundances of the Cr isotopes.[28] The natural abundance[28] of the Fe isotopes was relied on for correcting the signal intensity at a mass-to-charge ratio of 58 ($^{58}$Ni + $^{58}$Fe) for the isobaric interference by $^{58}$Fe. The isotope ratio measurements by ns-LA−MC-ICP-MS were performed following a standard-sample bracketing approach (SSB) using the geological reference material BCR-2G for external correction for the instrumental mass discrimination.

The accuracy and precision of the Fe isotope ratios are deteriorated if the signal intensities of sample and standard are not properly matched, as plasma loading affects the extent of mass bias.[29,30] By careful selection of laser spot size (beam diameter)[31] and repetition rate, rather than by adapting the laser energy density or by altering the source slit width of the MC-ICP-MS,[32] the signal intensity mismatch can be minimized.[15,29] BCR-2G was analyzed in line scanning mode with a circular laser spot size of 15 $\mu$m diameter, 20 shots per position, a laser energy density of 1.74 J $cm^{-2}$, and a laser repetition rate of 20 Hz. The concentrations of Fe in the samples were significantly different from that in BCR-2G, and thus the laser spot size (range: 10−30 $\mu$m) and laser repetition rate (range: 20−45 Hz) were adjusted for each sample to achieve signal intensities for samples and standard within ±10% after it had been demonstrated that, at least within the boundaries mentioned above, variation of these parameters does not affect the accuracy of the measured isotopes within the uncertainty of the method (Figure S2). The transient signal was acquired during 60 cycles with an integration time of 1.049


https://dx.doi.org/10.1021/acs.analchem.9b04029
Anal. Chem. 2020, 92, 3572−3580

s each. The internal precision for one individual measurement, i.e., the standard deviation (SD) of the average of $n$ integrations, improves when signals are integrated over longer times, e.g., 4.194 s; however, sample inhomogeneity can be identified more easily when a shorter integration time is used.

For Fe isotope ratio measurements by PN−MC-ICP-MS, a 100 $\mu$L min$^{-1}$ PFA concentric nebulizer mounted onto a dual spray chamber (with a cyclonic and a Scott-type subunit) was used for sample introduction. The Fe concentration was adjusted to 300 $\mu$g L$^{-1}$ in all solutions, and Ni (300 $\mu$g L$^{-1}$) was added as internal standard for correction for instrumental mass discrimination. The signal was acquired during 45 cycles with an integration time of 4.194 s and a cup configuration well established for PN (Table 1).[25,33] As pure Fe fractions (Fe was chromatographically isolated from the sample matrix) were used, no correction for the $^{54}$Cr−$^{54}$Fe isobaric interference was required, while the $^{58}$Fe and $^{58}$Ni nuclides were not considered. Measurements were performed in a SSB sequence using the IRMM-014 isotopic reference material as standard, and an in-house standard solution of Fe was measured every five samples for QA/QC purposes.

For sample introduction with either LA or PN, the results are reported in delta notation as per mil deviation (eq 1) and expressed relative to the Fe isotopic reference material IRMM-014.

$$\delta^{x}\mathrm{Fe} = [((^{x}\mathrm{Fe}/^{54}\mathrm{Fe})_{\mathrm{sample}}/(^{x}\mathrm{Fe}/^{54}\mathrm{Fe})_{\mathrm{IRMM\text{-}014}}) - 1] \times 1000 \quad (1)$$

Here $x$ is either 56 or 57.

**Data Processing for in Situ Fe Isotope Ratios.** To obtain precise and accurate Fe isotopes ratios from the transient signals obtained by ns-LA−MC-ICP-MS, three different strategies of data processing were investigated: the point-by-point (PBP), the integration, and the linear regression slope (LRS) method.[2,34] In the PBP method, the average of the isotope ratios measured over a certain range of acquisition points within the transient signal is calculated. In the integration method, isotope ratios were obtained by dividing the signal intensities integrated over the selected signal segment.[35] In the LRS method, the Fe isotope ratios were calculated as the slope of the best-fitting straight line (linear regression using the "least-squares" method) through the data points obtained by plotting the signal intensities for the isotopes involved versus one another.[36]

Instrumental mass discrimination was corrected for by means of a combination of internal correction using Ni as an internal standard introduced by PN following the approach of Baxter et al.[37] and external correction (SSB) using the geological reference material BCR-2G. The advantage of this approach for transient LA signals is that both Fe and Ni are collected simultaneously in static mode. As the Fe isotope ratios were initially measured relative to the BCR-2G reference material, the $\delta$-values were recalculated (following eq 2) and expressed relative to the IRMM-014 isotopic reference material for straightforward comparison with reported data.

$$\delta^{56}\mathrm{Fe}_{\mathrm{sample/IRMM\text{-}014}} = \delta^{56}\mathrm{Fe}_{\mathrm{sample/BCR\text{-}2G}} + \delta^{56}\mathrm{Fe}_{\mathrm{BCR\text{-}2G/IRMM\text{-}014}} \quad (2)$$

Here $\delta^{56}\mathrm{Fe}_{\mathrm{sample/BCR\text{-}2G}}$ is the (in situ) measured $\delta$-value of the sample relative to BCR-2G, and $\delta^{56}\mathrm{Fe}_{\mathrm{BCR\text{-}2G/IRMM\text{-}014}}$ is the $\delta$-value of BCR-2G relative to IRMM-014, as determined by PN−MC-ICP-MS.[14]

Statistical data analysis was performed using $t$-tests. The level of significance was established at $p < 0.05$.

## RESULTS AND DISCUSSION

**In Situ Fe Isotopic Analysis by ns-LA−MC-ICP-MS.** Iron isotope ratios were determined relative to the reference glass material BCR-2G, also used for tuning the instrument settings. Some additional information on the tuning is provided in the Supporting Information, which also includes partial peak profiles at mass-to-charge ratios of 54, 56, and 57 (Figure S3). After optimization, the signal intensity was ≥15 V for the $^{56}$Fe$^{+}$ ion and >0.3 V for the less abundant $^{54}$Fe and $^{57}$Fe isotopes. The Fe content in the glass reference materials ranged between 3 and 12 wt % FeO*, and thus signal matching was performed by adjusting the laser spot size and repetition rate. The sample surface was preablated at a laser energy density of 0.22 J cm$^{-2}$, which is lower than the ablation threshold of the glasses, for removal of potential surface contamination. Each sample was ablated during four different measurement sessions in which five line scan replicates were performed on each sample (30 s per line) covering different areas of the sample surface. The Ni internal standard solution (500 $\mu$g L$^{-1}$) was added to the sample aerosol via PN through one of the inlets of the glass T-piece, resulting in a signal intensity >12 V for the $^{58}$Ni$^{+}$ ion. Although Ni is also present in the glass reference materials (10−1000 $\mu$g g$^{-1}$),[22] its contribution to the overall signal was <0.5%.

The accuracy of the Fe isotope ratios is critically dependent on the correction for instrumental mass discrimination. BHVO-2G was used for optimization of the data acquisition and evaluation of the figures of merit attainable. After the strategies for data processing were applied, the reproducibility obtained for the BHVO-2G was 0.05‰ for the $\delta^{56}$Fe value and 0.07‰ for the $\delta^{57}$Fe value using the PBP method, 0.03‰ for the $\delta^{56}$Fe value and 0.06‰ for the $\delta^{57}$Fe value for the integration method, and finally the values obtained by the LRS method for $\delta^{56}$Fe and $\delta^{57}$Fe were 0.05‰ and 0.09‰ respectively (1 SD). The SD values were calculated from the average values obtained from each of the 4 measurement sessions (each consisting of 5 × 30 s ablation while line scanning). The signal contributions of the blanks were negligible. Thus, the integration method followed by the Baxter approach[36] to correct for mass discrimination provided the best internal and external precision, in line with the conclusion from earlier work on Sr and Pb isotopic analysis of archeological glass. This approach was applied to all samples. The results obtained for the seven MPI-DING and two USGS reference glasses are presented in Figure 1 in a three-isotope plot. As can be seen, the slope obtained is consistent with that for mass-dependent fractionation (1.5 for a $\delta^{57}$Fe−$\delta^{56}$Fe plot) within experimental uncertainty. This indicates that no interferences inducing a systematic bias occur. Table 2 shows the Fe isotopic compositions of the glass reference materials. The spatial variations in $\delta$-values within a single material ranged between 0.02 and 0.11‰ for $\delta^{56}$Fe and between 0.02 and 0.15‰ for the $\delta^{57}$Fe values (1 SD, $n$ = 4 measurement sessions, each covering 5 line scans). Moreover, the $\delta$-values obtained for the reference glasses are in excellent agreement with those reported in literature[14] obtained via fs-LA−MC-ICP-MS ($t$-test, $p > 0.05$).


https://dx.doi.org/10.1021/acs.analchem.9b04029
Anal. Chem. 2020, 92, 3572−3580

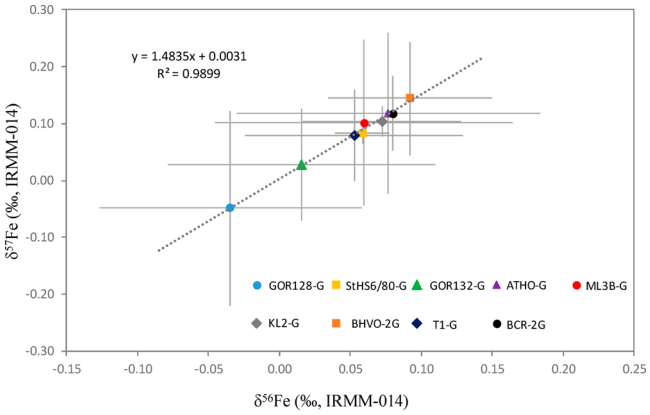


**Figure 1.** Three-isotope plot of Fe for the MPI-DING and USGS reference glasses analyzed by ns-LA−MC-ICP-MS. Error bars represent the reproducibility as SD of 4 measurement sessions ($n$ = 4 measurements sessions, each based on 5 line scans).

**Comparison of in Situ Analysis and Pneumatic Nebulization.** Iron isotope ratios were also determined via PN−MC-ICP-MS for six MPI-DING and one USGS glass reference material, to further validate the LA-based method for isotopic analysis. The concentrations of Fe and Ni were adjusted to 300 $\mu$g $L^{-1}$, resulting in signal intensities >14 V for the $^{56}Fe^+$ ion and >3 V for $^{60}Ni^+$ ion. The isotope ratio measurements were performed in a SSB sequence with IRMM-014 as bracketing standard. The $\delta$-values, obtained as the mean of four replicates from different measurement sessions, are shown in Table 2, and, as can be seen, the results are in good agreement with those obtained using ns-LA−MC-ICP-MS ($t$-test, $p$ > 0.05). No significant difference was established between $\delta$-values originating from both approaches. Moreover, the values obtained experimentally in this work also agree well with those reported in literature (Figure 2). To the best of the authors' knowledge, the Fe isotopic composition of the ATHO-G, the reference glass with the lowest FeO* content (3.27%), is characterized for the first time. The Fe isotopic composition of ATHO-G is consistent with the values reported for rhyolites.[38] As can be seen in Figure 3, the results obtained by ns-LA−MC-ICP-MS are in agreement with those obtained by PN−MC-ICP-MS despite the marked differences in matrix composition between glasses. By considering the Fe isotope ratio results obtained via PN-ICP-MS as "benchmark" data, the accuracy of the $\delta$-values obtained by ns-LA−MC-ICP-MS could be estimated by comparison. The bias between the results of both techniques varied from 0.001 to 0.022‰, with an average value of 0.012‰. The results also indicate that when using 5 line scans of 30 s each, MPI-DING and USGS reference glasses are sufficiently isotopically homogeneous and, thus, are suitable as external standards for the determination of the Fe isotope ratios by ns-LA−MC-ICP-MS (vide infra for a further discussion of their isotopic homogeneity).

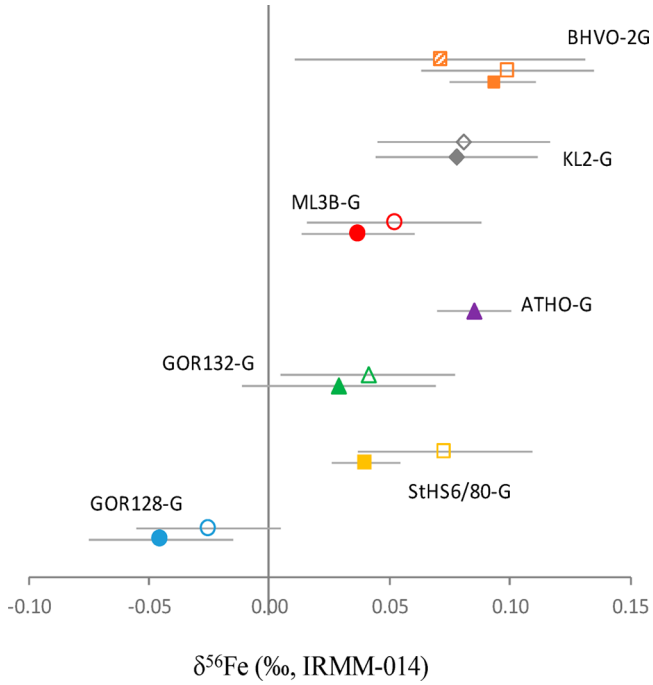


**Figure 2.** $\delta^{56}$Fe values for the geological reference glasses as obtained by ns-LA−MC-ICP-MS in this work and comparison with data reported in literature. Solid filled markers: $\delta$-values expressed relative to the Fe isotopic reference material IRMM-014 in this study. Data compiled from literature: open markers (data obtained by fs-LA−MC-ICP-MS, Oeser et al.[14]) and pattern filled marker ($\delta$-value obtained by PN−MC-ICP-MS, Chernonozhkin et al.[33]) expressed relative to the IRMM-014 isotopic reference material. Error bars represent reproducibility as provided in each study.

**Application to Glassy Cosmic Spherules.** Cosmic spherules are submillimeter-sized micrometeorites (typically round due to complete melting during atmospheric entry) and show a wide diversity in textures, compositions, and

**Table 2. Iron Isotope Ratio Data for MPI-DING and USGS Geological Reference Materials, Expressed (in ‰) Relative to the IRMM-014 Isotopic Reference Material, Obtained by ns-LA−MC-ICP-MS and PN−MC-ICP-MS ($n$ = 4 Measurements Sessions, Each Based on 5 Scan Lines)[a]**

| | | LA−MC-ICP-MS | | | | PN−MC-ICP-MS | | | |
|---|---|---|---|---|---|---|---|---|---|
| RM | FeO* (wt %) | $\delta^{56}$Fe | SD | $\delta^{57}$Fe | SD | $\delta^{56}$Fe | SD | $\delta^{57}$Fe | SD |
| GOR128-G | 9.81 | −0.035 | 0.092 | −0.049 | 0.172 | −0.045 | 0.035 | −0.058 | 0.036 |
| StHS6/80-G | 4.37 | 0.058 | 0.019 | 0.082 | 0.017 | 0.040 | 0.014 | 0.055 | 0.038 |
| GOR132-G | 10.1 | 0.015 | 0.094 | 0.028 | 0.099 | 0.029 | 0.044 | 0.043 | 0.027 |
| ATHO-G | 3.27 | 0.077 | 0.107 | 0.119 | 0.141 | 0.085 | 0.015 | 0.136 | 0.026 |
| ML3B-G | 10.9 | 0.059 | 0.105 | 0.102 | 0.146 | 0.037 | 0.023 | 0.069 | 0.070 |
| KL2-G | 10.7 | 0.072 | 0.055 | 0.103 | 0.027 | 0.078 | 0.034 | 0.122 | 0.040 |
| BHVO-2G | 11.3 | 0.092 | 0.057 | 0.144 | 0.100 | 0.093 | 0.018 | 0.135 | 0.025 |
| T1-G | 6.44 | 0.053 | 0.077 | 0.080 | 0.080 | | | | |
| BCR-2G | 12.4 | 0.080 | 0.046 | 0.118 | 0.066 | 0.085[a] | 0.016[a] | 0.127[a] | 0.028[a] |

[a]BCR-2G $\delta$-values and SD by PN−MC-ICP-MS were taken from ref 14. FeO* = all Fe as FeO, data from GeoReM.[23]


https://dx.doi.org/10.1021/acs.analchem.9b04029
Anal. Chem. 2020, 92, 3572−3580

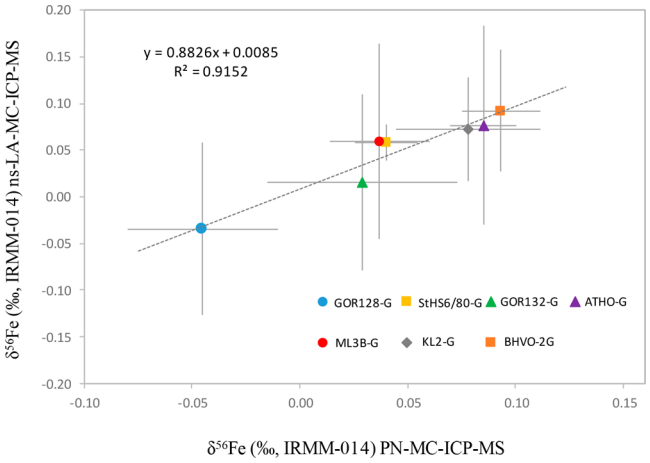


**Figure 3.** Comparison between the $\delta^{56}$Fe values obtained by ns-LA−MC-ICP-MS and by PN−MC-ICP-MS for the MPI-DING and USGS reference glasses (the dotted line corresponds to the regression line).

mineralogy. They can be divided into several chemical and textural groups: the silicate-rich spherules (S-type), the Fe-rich spherules (I-type), and the spherules which are mixtures (G-type). S-type cosmic spherules are composed mainly of mafic silicates and glass and are further subdivided according to their quench structures and chemical properties into the coarse-grained (CG), porphyritic olivine (Po), barred olivine (BO), cryptocrystalline (CC), glassy (V), and Ca−Al−Ti rich (CAT) subtypes.[39] These originally chondritic particles were fully melted during atmospheric passage and experienced considerable high-density phase ejection, e.g., of Fe−Ni metal, and evaporation. The latter is known to lead to significant degrees of isotope fractionation for moderately volatile elements such as O, Fe, and Ni. Several works have demonstrated a mass-dependent enrichment in the heavier Fe isotopes in cosmic spherules, which in some cases is up to several tens per mil,[40−42] with a precision typically on the order of 1‰.

In situ Fe isotopic analyses were performed for 13 glassy cosmic spherules (diameter range: 400−800 $\mu$m) by ns-LA−MC-ICP-MS. They were selected due to their vitreous texture and relatively uniform distribution of major elements (SEM, Figure 4). Glassy spherules are often transparent, and their color is mainly determined by the Fe content (between 0.86 and 18.8 wt % FeO* here); the lower the Fe content, the lighter the color. To ensure an adequate correction relative to BCR-2G, the Fe signal intensities were matched by adjusting the laser spot size and repetition rate for each glassy cosmic spherule individually. All samples were preablated to remove any surface contamination, and ablation was done according to line scan replicates, covering the entire surface of the sample. Table 3 summarizes the Fe content and the Fe isotope ratio data of each sample, originating from three different measurement sessions. The $\delta^{56}$Fe values ranged from 0.25 to 24.99‰, while the $\delta^{57}$Fe values vary between 0.38 and 37.11‰. These values indicate a wide range of Fe isotope fractionation during atmospheric entry. The extent of Fe isotope fractionation is higher in the samples with low Fe content than in those with a more elevated Fe content, as is expected in evaporation processes. The reproducibility obtained for the $\delta$-values was between 0.03 and 0.17‰ and between 0.07 and 0.29‰ for $\delta^{56}$Fe and for $\delta^{57}$Fe, respectively, when calculated as 1 SD, for 3 measurements sessions ($n$ = 3). The $\delta$Fe values are in line with those reported in literature for (other) cosmic spherules.[40,41] Figure 5 shows a comparison between $\delta$-values determined by ns-LA−MC-ICP-MS and PN−MC-ICP-MS for eight of the glassy cosmic spherules. In general, in situ data were in agreement with the $\delta^{56}$Fe values obtained by PN−MC-ICP-MS. However, for the highest $\delta^{56}$Fe values, a bias is seen between the corresponding LA/PN data. It cannot be excluded that the large difference between the $\delta^{56}$Fe value for these samples and that for the bracketing standard contributes to this bias. However, examination of the variation of the isotope ratio measurement result along a single ablation line reveals what is probably the real cause of this bias, i.e., isotopic inhomogeneity >1 ‰ in some micrometeorites. Figure 6 shows an example of the $\delta^{56}$Fe value variation along two ablation lines for the BCR-2G reference material used as external standard and for two samples. For BCR-2G, it can be seen that the variation in $\delta^{56}$Fe along each ablation line is within ±0.1 ‰, while the results for the two lines show an excellent match. This further proves the isotopic homogeneity of this reference material. For sample WF1202B-012, the results as obtained along the two ablation lines overlap, but the variation in $\delta^{56}$Fe along each ablation line is of the order of ±0.5 ‰ indicative of a somewhat larger isotopic heterogeneity. For WF1202B-005, finally, the isotope ratio results are different between the two ablation lines, while the variation along one such line even amounts to 2‰, indicating more pronounced isotopic heterogeneity. As a result of the way in which they are calculated, this is not reflected in the SDs reported in Table 3. In an attempt to express this

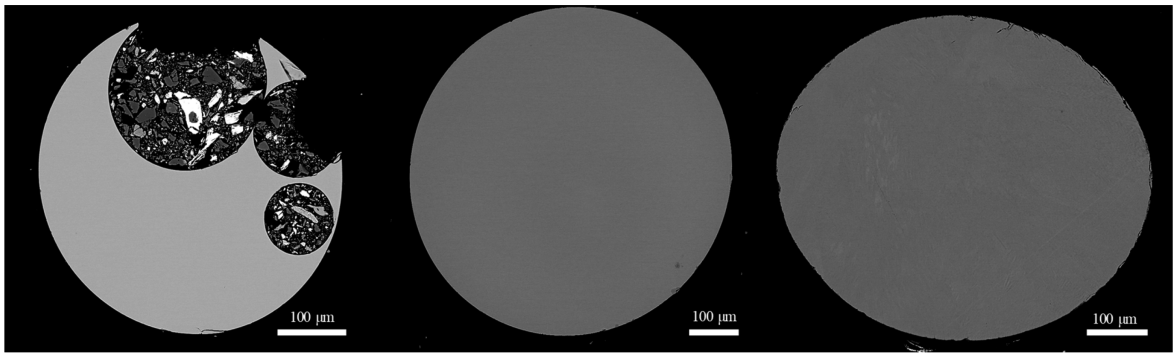


**Figure 4.** Backscattered electron images for a selection of the glassy cosmic spherules characterized in this work. From left to right, particles WF1202B-0004, 0019 and 0005, which exhibit low, moderate, and high enrichments in the heavier Fe isotopes ($\delta^{56}$Fe of 0.29, 12.82, 24.99‰, respectively). While the polished sections of WF1202B-0019 and 0005 do not contain any vesicles or high-density phases, glassy cosmic spherule WF1202B-0004 exhibits three large vesicles filled with background sediment. Scale bar = 100 $\mu$m.


https://dx.doi.org/10.1021/acs.analchem.9b04029
Anal. Chem. 2020, 92, 3572−3580

**Table 3. Fe Content and Isotope Ratio Data (δ-Values in ‰) for 13 Glassy Cosmic Spherules As Determined by EMPA, ns-LA−MC-ICP-MS, and PN−MC-ICP-MS, Respectively[a]**

| | | | LA−MC-ICP-MS | | | | | | PN−MC-ICP-MS | | | |
|---|---|---|---|---|---|---|---|---|---|---|---|---|
| cosmic spherule | diameter (μm) | FeO* (wt %) | $\delta^{56}$Fe | $SD_{internal}$ | SD | $\delta^{57}$Fe | $SD_{internal}$ | SD | $\delta^{56}$Fe | SD | $\delta^{57}$Fe | SD |
| WF1202B-0001 | 622 | 3.88 | 1.23 | 0.11 | 0.10 | 1.59 | 0.15 | 0.16 | | | | |
| WF1202B-0004 | 501 | 12.2 | 0.29 | 0.08 | 0.03 | 0.43 | 0.13 | 0.09 | 0.14 | 0.05 | 0.19 | 0.04 |
| WF1202B-0005 | 622 | 3.72 | 24.99 | 0.31 | 0.16 | 37.11 | 0.41 | 0.25 | 22.93 | 0.03 | 34.14 | 0.04 |
| WF1202B-0009 | 527 | 8.86 | 4.76 | 0.14 | 0.17 | 7.08 | 0.18 | 0.12 | 4.38 | 0.03 | 6.53 | 0.01 |
| WF1202B-0010 | 764 | 1.64 | 5.13 | 0.07 | 0.05 | 7.67 | 0.15 | 0.11 | | | | |
| WF1202B-0012 | 512 | 17.9 | 3.92 | 0.12 | 0.05 | 5.61 | 0.13 | 0.06 | 3.79 | 0.03 | 5.65 | 0.04 |
| WF1202B-0017 | 791 | 15.1 | 3.56 | 0.09 | 0.11 | 5.24 | 0.16 | 0.29 | 3.31 | 0.03 | 5.00 | 0.01 |
| WF1202B-0019 | 712 | 12.1 | 12.82 | 0.05 | 0.03 | 18.88 | 0.14 | 0.16 | 12.33 | 0.01 | 18.42 | 0.03 |
| WF1202B-0020 | 620 | 9.04 | 14.16 | 0.20 | 0.08 | 21.16 | 0.29 | 0.20 | 13.14 | 0.01 | 19.66 | 0.04 |
| WF1202B-0021 | 551 | 18.8 | 0.25 | 0.07 | 0.08 | 0.38 | 0.14 | 0.15 | | | | |
| WF1202B-0024[b] | 635 | 8.43 | 3.16 | 0.21 | 0.09 | 4.87 | 0.33 | 0.20 | 2.25 | 0.01 | 3.59 | 0.01 |
| WF1202B-0039 | 439 | 18.37 | 0.93 | 0.07 | 0.04 | 1.35 | 0.10 | 0.07 | | | | |
| WF1202B-0048 | 498 | 0.86 | 16.38 | 0.11 | 0.12 | 24.48 | 0.17 | 0.19 | | | | |

[a]The precision is expressed as standard deviation for $n = 3$ measurements sessions. $SD_{internal}$ corresponds to the internal standard deviation per line via in situ analysis. FeO* represents all Fe. [b]High Ca content.

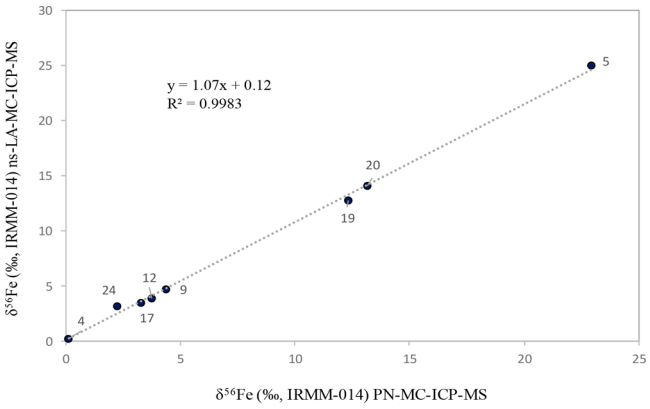


**Figure 5.** $\delta^{56}$Fe values for glassy cosmic spherules obtained by ns-LA−MC-ICP-MS and by PN−MC-ICP-MS. The numbering in the figure refers to the sample designations. Error bars (1 SD for $n = 3$ measurements sessions) are smaller than the symbols used (the dotted line corresponds to the regression line).

inhomogeneity quantitatively, we have also calculated the SD along a single line ($SD_{internal}$), but even this does not reflect this along-line variation very well. Also for WF1202B-0020 and WF1202B-0024, such isotopic heterogeneity could be detected. The shifted value for WF1202B-0024 cosmic spherule, on the other hand, may also be due to its matrix, as it shows the highest calcium content.

As previously pointed out, glass reference materials can be appropriately used as bracketing standard for in situ Fe isotopic analysis by ns-LA−MC-ICP-MS. To confirm this, also the ML3B-G reference material was used as bracketing standard for Fe isotopic analysis of four of the glassy cosmic spherules via ns-LA−MC-ICP-MS. In this case, the Fe signal intensities were matched relative to ML3B-G, and the δ-values were recalculated relative to IRMM-014 after its isotopic characterization by PN−MC-ICP-MS. In situ isotopic analysis of the samples yielded $\delta^{56}$Fe values of 4.55 ± 0.21‰, 13.08 ± 0.08‰, 14.10 ± 0.06‰, and 3.41 ± 0.04‰, while $\delta^{57}$Fe values were 6.77 ± 0.16‰, 19.32 ± 0.17‰, 21.00 ± 0.05‰, and 4.93 ± 0.15‰ for sample WF1202B-9, WF1202B-19, WF1202B-20, and WF1202B-24, respectively. These results were in agreement with those presented in Table 3, indicating the suitability of most glass reference materials as external standard in in situ Fe isotopic analysis of glassy cosmic spherules by ns-LA−MC-ICP-MS.

## ■ CONCLUSIONS

Iron isotope ratios were determined for glass reference materials and micrometer-sized glassy cosmic spherules via ns-LA−MC-ICP-MS. The integration method (isotope ratios obtained by dividing the corresponding signal intensities integrated over the selected signal segment) was selected for extracting the Fe isotope ratios from the transient ion signals, while the bias caused by instrumental mass discrimination was corrected for by a combination of internal (using Ni) and

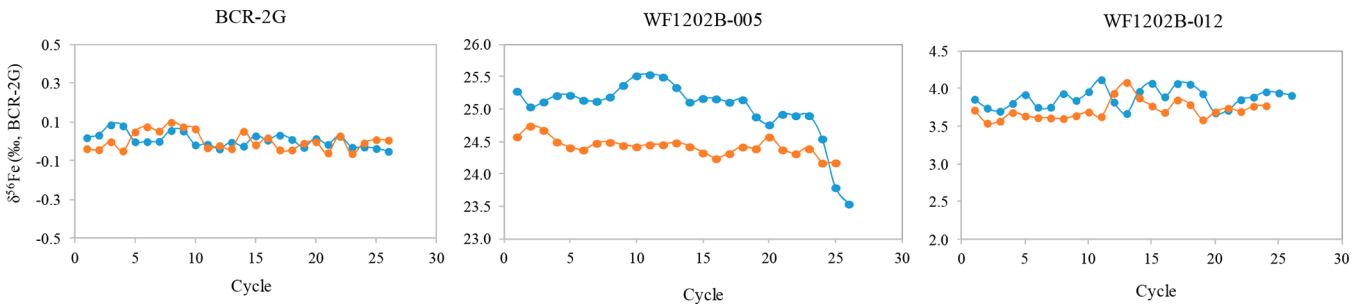


**Figure 6.** Individual $\delta^{56}$Fe values as obtained by ns-LA−MC-ICP-MS along two lines; values for BCR-2G and two glassy cosmic spherules.


https://dx.doi.org/10.1021/acs.analchem.9b04029
Anal. Chem. 2020, 92, 3572−3580

external standardization. For glass RMs, the δFe values obtained by ns-LA−MC-ICP-MS were in agreement with those obtained by PN−MC-ICP-MS and with earlier values reported in literature. There was an overall agreement between the ns-LA−MC-ICP-MS and the PN−MC-ICP-MS results for the cosmic spherules as well; the larger bias observed for some of these samples was tentatively attributed to isotopic heterogeneity. All glassy cosmic spherules were enriched in the heavier Fe isotopes ($\delta^{56}$Fe ranging from 0.3 to 25‰) compared to the glass reference materials measured here. As the geological reference materials and cosmic spherules show a large range of Fe concentrations, the in situ method developed is relatively matrix-independent. These results demonstrate that ns-LA−MC-ICP-MS is a suitable technique for in situ Fe isotopic analysis of glassy cosmic spherules, thus enabling pioneering research in the fields of the Earth and planetary sciences with instrumentation that is relatively affordable and, thus, within reach of more laboratories.

## ■ ASSOCIATED CONTENT

### Supporting Information

The Supporting Information is available free of charge at https://pubs.acs.org/doi/10.1021/acs.analchem.9b04029.

Scheme of the experimental setup for in situ analysis (Figure S1); nanosecond-LA−MC-ICP-MS $^{56}$Fe/$^{54}$Fe isotope ratio results for BHVO-2G obtained using various combinations of laser spot diameter and laser repetition frequency (Figure S2); partial spectrum obtained via a mass scan of the left side of the Fe peaks obtained at (pseudo) medium resolution for BCR-2G analyzed using ns-LA−MC-ICP-MS (Figure S3) (PDF)

## ■ AUTHOR INFORMATION


### Corresponding Author

**Frank Vanhaecke** − *Ghent University, Department of Chemistry, Atomic & Mass Spectrometry-A&MS research unit, 9000 Ghent, Belgium;* orcid.org/0000-0002-1884-3853; Email: frank.vanhaecke@ugent.be

### Authors

**Claudia González de Vega** − *Ghent University, Department of Chemistry, Atomic & Mass Spectrometry-A&MS research unit, 9000 Ghent, Belgium*

**Marta Costas-Rodríguez** − *Ghent University, Department of Chemistry, Atomic & Mass Spectrometry-A&MS research unit, 9000 Ghent, Belgium;* orcid.org/0000-0002-8159-9961

**Thibaut Van Acker** − *Ghent University, Department of Chemistry, Atomic & Mass Spectrometry-A&MS research unit, 9000 Ghent, Belgium;* orcid.org/0000-0002-0649-7228

**Steven Goderis** − *Vrije Universiteit Brussel (VUB), Analytical, Environmental and Geo-Chemistry (AMGC), 1050 Brussels, Belgium;* orcid.org/0000-0002-6666-7153

Complete contact information is available at: https://pubs.acs.org/10.1021/acs.analchem.9b04029


### Notes

The authors declare the following competing financial interest(s): Teledyne CETAC Technologies funded the Ph.D. grant of T.V.A. (promoter: F.V.) under contract A15-TT-0627. F.V. is co-inventor of patent WO2016042165A1, on which part of the technology of the ablation cell used in this work is based. The A&MS research group at Ghent University has licensed intellectual property to Teledyne CETAC Technologies.

## ■ ACKNOWLEDGMENTS

C.G.d.V. acknowledges the grant received from the Marie Curie Clarín-COFUND project of the Principality of Asturias and the European Union. S.G. and F.V. thank FWO and FNRS for financial support through the EOS-Excellence of Science programme. F.V. acknowledges BOF-UGent for financial support. M.C.-R. thanks FWO-Vlaanderen for the postdoctoral grant. The authors acknowledge Teledyne CETAC Technologies Inc. for financial and logistic support.

## ■ REFERENCES


(1) Goderis, S.; Chakrabarti, R.; Debaille, V.; Kodolányi, J. *J. Anal. At. Spectrom.* **2016**, *31*, 841−862.
(2) Yang, L. *Mass Spectrom. Rev.* **2009**, *28*, 990−1011.
(3) Balcaen, L.; Moens, l.; Vanhaecke, F. *Spectrochim. Acta, Part B* **2010**, *65*, 769−786.
(4) Beard, B. L.; Johnson, C. M. *Rev. Mineral. Geochem.* **2004**, *55*, 319−357.
(5) Poitrasson, F.; Zambardi, T.; Magna, T.; Neal, C. R. *Geochim. Cosmochim. Acta* **2019**, *267*, 257−274.
(6) Craddock, P. R.; Dauphas, N. *Geostand. Geoanal. Res.* **2011**, *35*, 101−123.
(7) Chernonozhkin, S. M.; Goderis, S.; Costas-Rodríguez, M.; Claeys, P.; Vanhaecke, F. *Geochim. Cosmochim. Acta* **2016**, *186*, 168−188.
(8) Dauphas, N.; John, S. G.; Rouxel, O. *Rev. Mineral. Geochem.* **2017**, *82*, 415−510.
(9) Dauphas, N.; Pourmand, A.; Teng, F.-Z. *Chem. Geol.* **2009**, *267*, 175−184.
(10) Russo, R. E.; Mao, X.; Gonzalez, J. J.; Zorba, V.; Yoo, J. *Anal. Chem.* **2013**, *85*, 6162−6177.
(11) Horn, I.; von Blanckenburg, F. *Spectrochim. Acta, Part B* **2007**, *62*, 410−422.
(12) Horn, I.; von Blanckenburg, F.; Schoenberg, R.; Steinhoefel, G.; Markl, G. *Geochim. Cosmochim. Acta* **2006**, *70*, 3677−3688.
(13) Steinhoefel, G.; Horn, I.; von Blanckenburg, F. *Chem. Geol.* **2009**, *268*, 67−73.
(14) Oeser, M.; Weyer, S.; Horn, I.; Schuth, S. *Geostand. Geoanal. Res.* **2014**, *38*, 311−328.
(15) Chernonozhkin, S. M.; Weyrauch, M.; Goderis, S.; Oeser, M.; McKibbin, S. J.; Horn, I.; Hecht, L.; Weyer, S.; Claeys, P.; Vanhaecke, F. *Geochim. Cosmochim. Acta* **2017**, *217*, 95−111.
(16) Košler, J.; Pedersen, R. B.; Kruber, C.; Sylvester, P. J. *J. Anal. At. Spectrom.* **2005**, *20*, 192−199.
(17) d'Abzac, F.-X.; Beard, B. L.; Czaja, A. D.; Konishi, H.; Schauer, J. J.; Johnson, C. M. *Anal. Chem.* **2013**, *85*, 11885−11892.
(18) Claverie, F.; Hubert, A.; Berail, S.; Donard, A.; Pointurier, F.; Pécheyran, C. *Anal. Chem.* **2016**, *88*, 4375−4382.
(19) Hirata, T.; Hayano, Y.; Ohno, T. *J. Anal. At. Spectrom.* **2003**, *18*, 1283−1288.
(20) Van Ham-Meert, A.; Chernonozhkin, S. M.; Van Malderen, S.; Van Acker, T.; Vanhaecke, F.; Degryse, P. *Geostand. Geoanal. Res.* **2018**, *42*, 223−238.
(21) Zheng, X.-Y.; Beard, B. L.; Johnson, C. M. *J. Anal. At. Spectrom.* **2018**, *33*, 68−83.
(22) Sio, C. K. I.; Dauphas, N.; Teng, F.-Z.; Chaussidon, M.; Helz, R. T.; Roskosz, M. *Geochim. Cosmochim. Acta* **2013**, *123*, 302−321.
(23) Jochum, K. P.; Nohl, U.; Herwig, K.; Lammel, E.; Stoll, B.; Hofmann, A. W. *Geostand. Newsl.* **2005**, *29*, 333−338.
(24) Goderis, S.; Soens, B.; Huber, M. S.; McKibbin, S.; van Ginneken, M.; Van Maldeghem, F.; Debaille, V.; Greenwood, R. C.; Franchi, I. A.; Cnudde, V.; Van Malderen, S.; Vanhaecke, F.; Koeberl, C.; Topa, D.; Claeys, Ph. *Geochim. Cosmochim. Acta* **2020**, *270*, 112.

(25) Anoshkina, Y.; Costas-Rodriguez, M.; Vanhaecke, F. *J. Anal. At. Spectrom.* **2017**, *32*, 314−321.
(26) Vanhaecke, F.; Van Malderen, S. J. M. *Laser Ablation Probe*. US2017/0299522A1, 2017.
(27) Van Malderen, S. J. M.; van Elteren, J. T.; Vanhaecke, F. *J. Anal. At. Spectrom.* **2015**, *30*, 119−125.
(28) Meija, J.; Coplen, T. B.; Berglund, M.; Brand, W. A.; De Bièvre, P.; Gröning, M.; Holden, N. E.; Irrgeher, J.; Loss, R. D.; Walczyk, T.; Prohaska, T. *Pure Appl. Chem.* **2016**, *88*, 293−306.
(29) Lin, J.; Liu, Y.; Tong, X.; Zhu, L.; Zhang, W.; Hu, Z. *J. Anal. At. Spectrom.* **2017**, *32*, 834−842.
(30) Albarède, F.; Albalat, E.; Télouk, P. *J. Anal. At. Spectrom.* **2015**, *30*, 1736−1742.
(31) Devulder, V.; Gerdes, A.; Vanhaecke, F.; Degryse, P. *Spectrochim. Acta, Part B* **2015**, *105*, 116−120.
(32) le Roux, P. J. *J. Anal. At. Spectrom.* **2010**, *25*, 1033−1038.
(33) Chernonozhkin, S. M.; Costas-Rodríguez, M.; Claeys, P.; Vanhaecke, F. *J. Anal. At. Spectrom.* **2017**, *32*, 538−547.
(34) Kappel, S.; Boulyga, S. F.; Dorta, L.; Günther, D.; Hattendorf, B.; Koffler, D.; Laaha, G.; Leisch, F.; Prohaska, T. *Anal. Bioanal. Chem.* **2013**, *405*, 2943−2955.
(35) Günther-Leopold, I.; Wernli, B.; Kopajtic, Z.; Günther, D. *Anal. Bioanal. Chem.* **2004**, *378*, 241−249.
(36) Fietzke, J.; Liebetrau, V.; Günther, D.; Gürs, K.; Hametner, K.; Zumholz, K.; Hansteen, T. H.; Eisenhauer, A. *J. Anal. At. Spectrom.* **2008**, *23*, 955−961.
(37) Baxter, D. C.; Rodushkin, I.; Engström, E.; Malinovsky, D. *J. Anal. At. Spectrom.* **2006**, *21*, 427−430.
(38) Du, D.-H.; Wang, X.-L.; Yang, T.; Chen, X.; Li, J.-Y.; Li, W. *Geochim. Cosmochim. Acta* **2017**, *218*, 58−72.
(39) Genge, M. J.; Engrand, C.; Gounelle, M.; Taylor, S. *Meteorit. Planet. Sci.* **2008**, *43*, 497−515.
(40) Alexander, C. M. O'D.; Taylor, S.; Delaney, J. S.; Ma, P.; Herzog, G. F. *Geochim. Cosmochim. Acta* **2002**, *66*, 173−183.
(41) Taylor, S.; Alexander, C. M. O'D.; Delaney, J.; Ma, P.; Herzog, G. F.; Engrand, C. *Geochim. Cosmochim. Acta* **2005**, *69*, 2647−2662.
(42) Engrand, C.; Mckeegan, K. D.; Leshin, L. A.; Herzog, G. F.; Schnabel, C.; Nyquist, L. E.; Brownlee, D. E. *Geochim. Cosmochim. Acta* **2005**, *69*, 5365−5385.


https://dx.doi.org/10.1021/acs.analchem.9b04029
*Anal. Chem.* 2020, 92, 3572−3580